

# Effects of a Powered Knee-Ankle Prosthesis on Amputee Hip Compensations: A Case Series

Toby Elery, *Student Member, IEEE*, Siavash Rezazadeh, *Member, IEEE*, Emma Reznick, *Student Member, IEEE*, Leslie Gray, and Robert D. Gregg, *Senior Member, IEEE*

**Abstract**—Transfemoral amputee gait often exhibits compensations due to the lack of ankle push-off power and control over swing foot position using passive prostheses. Powered prostheses can restore this functionality, but their effects on compensatory behaviors, specifically at the residual hip, are not well understood. This paper investigates residual hip compensations through walking experiments with three transfemoral amputees using a low-impedance powered knee-ankle prosthesis compared to their day-to-day passive prosthesis. The powered prosthesis used impedance control during stance for compliant interaction with the ground, a time-based push-off controller to deliver high torque and power, and phase-based trajectory tracking during swing to provide user control over foot placement. Experiments show that when subjects utilized the powered ankle push-off, less mechanical pull-off power was required from the residual hip to progress the limb forward. Overall positive work at the residual hip was reduced for 2 of 3 subjects, and negative work was reduced for all subjects. Moreover, all subjects displayed increased step length, increased propulsive impulses on the prosthetic side, and improved impulse symmetries. Hip circumduction improved for subjects who had previously exhibited this compensation on their passive prosthesis. These improvements in gait, especially reduced residual hip power and work, have the potential to reduce fatigue and overuse injuries in persons with transfemoral amputation.

**Index Terms**—rehabilitation robotics, powered prostheses, gait compensations, low-impedance actuators

## I. INTRODUCTION

**P**ASSIVE or semi-active prostheses are commonly used to restore gait after a lower-limb amputation, however the resulting gait is often asymmetric and compensatory in nature [1], [2]. Clinicians typically prescribe and configure prostheses to reduce such asymmetries and compensations, with the goal of achieving more normative gait patterns. Semi-active prostheses such as the C-Leg improve gait by utilizing microprocessors to control the damping of joints via small actuators that manipulate hydraulic valves during the user's gait [3]. This design approach allows for a single product to be easily adaptable to a variety of subjects, environments,

T. Elery is with the Departments of Mechanical Engineering and Bioengineering, University of Texas at Dallas, Richardson, TX, 75080 USA. S. Rezazadeh is with the Department of Mechanical Engineering, University of Denver, Denver, CO, 80208 USA. L. Gray is with the School of Health Professions, University of Texas Southwestern Medical Center, Dallas, TX 75390 USA. E. Reznick and R. D. Gregg are with the Department of Electrical Engineering and Computer Science and the Robotics Institute, University of Michigan, Ann Arbor, MI, 48109 USA. e-mail: (rdgregg@umich.edu).

This work was supported by the National Institute of Child Health & Human Development of the NIH under Award Number R01HD094772. This work was also supported by NSF Awards 1734600 / 1949346. The content is solely the responsibility of the authors and does not necessarily represent the official views of the NIH or NSF. Robert D. Gregg, IV, Ph.D., holds a Career Award at the Scientific Interface from the Burroughs Wellcome Fund.

and tasks. However, semi-active devices can only dissipate energy from the user, and cannot exert net positive work like a biological leg. In particular, these prostheses lack ankle push-off power during late stance and knee flexion during early stance [4], [5]. This results in a gait that exhibits compensations, such as increased joint work at the hip to accommodate missing work at the knee and ankle [6], [7], and asymmetric kinematic deviations from normative gait, such as increased hip circumduction or decreased hip flexion [6], [8]. Prolonged repetition of these compensations can have detrimental effects on a person's health, comfort, and pain levels [6], [9]. For instance, asymmetries in gait can lead to knee osteoarthritis [10], muscle atrophy [11], and chronic back pain [11]. Mitigating compensatory behaviors and asymmetries should be a driving factor when designing prostheses to aid those with limb loss. Although anatomical changes associated with limb amputation may make it impossible to completely eliminate these behaviors, powered prostheses have the potential to reduce gait deviations related to leg biomechanics.

In the emerging field of powered prosthetic legs [12]–[14], some devices have been able to increase symmetry in joint kinematics [15], [16] and load distribution [17], and reduce muscle activity in the lower back [18]. Although great progress has been made with these devices, there is still a lack of evidence that powered prostheses can decrease amputee hip compensations. Rezazadeh et al. observed that a powered prosthesis reduced vaulting and circumduction in one transfemoral amputee [15]. However, the rigid actuation scheme of the prosthesis resulted in toe-stubbing, which can lead to other hip compensations like hip-hiking or increased hip work. Most powered prostheses implement similar stiff actuation styles, which have high mechanical impedance. This means that they require large load torques to backdrive the motor; also described as having low backdrivability [19], [20]. This design philosophy limits the actuator's force and position bandwidth, limiting highly dynamic portions of gait [15], [21], [22]. Push-off, for example, involves a rapid change from high-torque at low-speed to low-torque at high-speed, which requires very high bandwidth. Therefore, designs that limit this bandwidth risk stubbing the toe during the swing phase and reducing push-off power, which is critical in returning functionality to persons with limb loss, and is a leading factor in gait asymmetry and compensations [23]. Furthermore, these limitations have shown to be crucial in how persons with limb loss load their intact limb, which can have long term detrimental effects on their joints [6], [17].

As a starting point to address these challenges, we re-

cently designed a powered knee-ankle prosthesis with low mechanical impedance, or high-backdrivability [24], [25]. This prosthesis displays several practical benefits, such as reduced overall energy consumption and acoustic noise levels, but also has benefits related to control and power density. Preliminary tests proved that the intrinsic impedance and unmodeled dynamics of the actuators were sufficiently small to control joint impedance without torque feedback. Similarly, the actuators demonstrated precise position tracking capabilities throughout benchtop and walking experiments. Testing demonstrated increased actuator torque, power, and position bandwidth compared to high-impedance actuators. The increased capabilities of this prosthesis, coupled with the range of applicable control schemes available, suggest that this device may be uniquely suited to meet the varying needs of gait.

To further exploit the capabilities and flexibility of this style of actuation, this paper introduces a control scheme that utilized both its impedance and trajectory tracking abilities. Impedance control is utilized during the stance phase to provide biomimetic forceful interaction with the ground, as shown in [21]. Time-based kinematic control is used during push-off, when the foot is still on the ground, to promote large plantarflexion power and forward propulsion. Lastly, a time-invariant kinematic control method, based on a phase variable derived from thigh motion [19], is utilized to provide user synchronization across walking speeds and kinematic variations. Although previous implementations of time-invariant kinematic control have been limited to stiff actuation styles, this method has demonstrated promising results with both rhythmic and nonrhythmic activities, including more symmetric gait and reduced compensations in one user [15].

We expect that the combination of this actuation and control scheme will lead to reductions in residual hip kinematic and kinetic compensations, in addition to increased kinematic and force-related symmetry between the prosthetic and intact leg. Specifically, we predict the increased force bandwidth inherent to this style of actuation [25]–[27], coupled with time-based kinematic control during push-off, can be leveraged to provide more push-off (or plantarflexion) power at the ankle. Since increased push-off power is correlated to an increase in propulsive impulse, it is possible to improve symmetry between the braking and propulsive impulses of the prosthesis [28], [29]. This can lead to improved symmetry between the prosthetic limb’s propulsive impulse and the intact limb’s braking impulse, which has been linked to reduced power at the residual hip [4], [23], [30]. As a result, we expect to see reduced mechanical power and work at the residual hip, which is linked to reduced muscle and metabolic work [31], [32] and could potentially mitigate fatigue and long term injuries [9]. We also expect that the increased position bandwidth should allow quick ankle and knee flexion between terminal stance and mid-swing for increased toe-clearance [15], reducing the need for compensations such as circumduction. The phase-based swing controller can ensure that essential joint kinematics providing toe-clearance are correctly timed for each step, further diminishing the need for circumduction. Noting that the root causes and extent of circumduction are highly individualistic, this study only intends to address

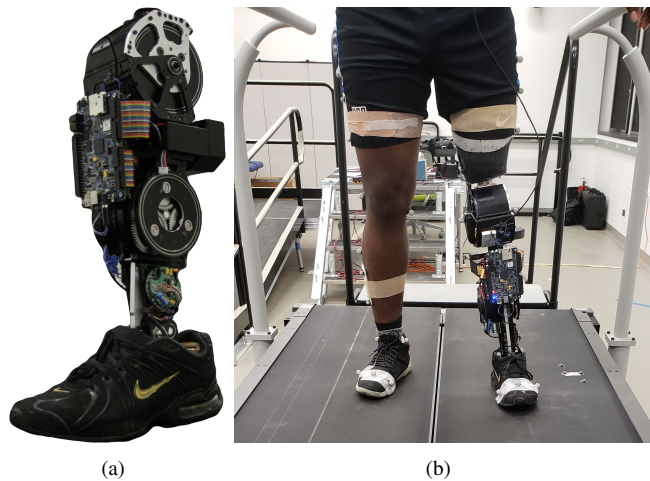


Fig. 1. (a) The powered prosthesis with high-torque, low-impedance actuators used in experimentation. (b) Experimental setup, including a subject wearing the powered prosthesis while standing on the instrumented treadmill and wearing reflective markers on their lower body.

compensations associated with prosthetic leg biomechanics.

This study investigates the ability of a powered prosthetic leg to positively impact residual hip compensations in three subjects with an amputation at the transfemoral level, compared to their gait while wearing their daily passive prosthesis. Methodologies relating to the hardware, experimental protocol, and powered prosthetic control are discussed in Section II. The effects on symmetries and compensations are presented in Section III and discussed in Section IV.

## II. METHODS

### A. Hardware

This study used the powered transfemoral prosthesis in Fig. 1, which was designed in [25] with high-torque, low-impedance actuators at the knee and ankle. Each actuator has an ILM 85x26, frameless, brushless, DC motor kit (Robodrive, Seefeld, Germany), and custom a 22:1 single-stage stepped-planet compound planetary gear transmission. A R80/80 Solo Gold Twitter motor driver (Elmo Motion Control, Petah Tikva, Israel) is used in low-level current control. Optical quadrature encoders, E5 (US Digital, Vancouver, WA), are used for motor position feedback to the motor drivers and the controller. To measure thigh angle, a 3DM-CX5-25 Inertial Measurement Unit, or IMU (LORD Microstrain, Williston, VT), is attached to the top hinge of the knee actuator. A M3564F 6-axis load cell (Sunrise Instruments, Nanning, China) is located below the ankle joint axis to detect ground contact. Mounted below the load cell is a size 28 (cm) Pacifica LP prosthetic foot (Freedom Innovations, Irvine, CA, USA). All sensors interface with the system’s microcontroller, a myRIO (National Instruments, Austin, TX). The controller presented in Section II-C is implemented in LabVIEW and imported onto the myRIO. The leg is powered through four onboard LiPo batteries, TP870-3SR70 (Thunder Power, Las Vegas, NV), connected in series. The overall mass of the leg is 6.09 kg, not including the cosmetic foot shell or shoe.

TABLE I  
SUBJECT INFORMATION AND MEASUREMENTS

	TF1	TF2	TF3
Weight (kg)	77.3	74.9	104.0
Age (yrs)	33	39	62
Height (m)	1.75	1.72	1.80
Residual Thigh Length (m)	0.23	0.31	0.30
Amputated Side	Left	Left	Left
Years Post Amputation	13	10	15
Day-to-day Knee Prosthesis	Ottobock 3R60	LegWorks All-Terrain	Ossur Rheo XC
Day-to-day Ankle/Foot Prosthesis	Ottobock Axtion 1E56	Ottobock Axtion 1E56	Ossur Proflex XC
Day-to-day Prosthesis Mass (kg)	4.0	2.9	4.3

TABLE II

TRIAL SPECIFIC INFORMATION: SUBJECT SELF-SELECTED WALKING SPEED, NUMBER OF STRIDES USED WHEN PRESENTING DATA (N), AND NUMBER OF STRIDES REJECTED AS OUTLIERS (R).

Subject	Speed (m/s)	Powered		Passive	
		N	R	N	R
TF1	Slow: 0.9	26	2	25	22
	Normal: 1.1	31	0	37	0
	Fast: 1.3	45	5	39	0
TF2	Slow: 0.8	35	3	36	0
	Normal: 1.0	38	2	40	0
	Fast: 1.2	42	0	36	0
TF3	Slow: 0.8	28	5	25	0
	Normal: 1.0	37	0	27	0
	Fast: 1.2	34	0	31	0

### B. Experimental Protocol

The following experimental protocol was approved by the Institutional Review Boards of the University of Texas at Dallas, the University of Texas Southwestern Medical Center, and the University of Michigan; IRB 17-128, approved on July 19, 2019. A clinical researcher, who is a practicing, certified, and licensed prosthetist, was present during all experimentation. Three subjects with amputations at the transfemoral (above-knee) level, identified as TF1, TF2, and TF3, were recruited through the clinical researcher, with written informed consent and without bias of race or gender.

The clinical researcher fit the powered prosthesis to each subject, ensuring the knee height, knee rotation, and foot progression angle were properly aligned. Note that the large diameter of the actuators may limit the alignment of the prosthetic and intact knee height, for subjects with long residual limbs and sockets, such as TF3. Anatomical and subject-specific information is presented in Table I. A training session was conducted with each subject before experimentation with the powered prosthesis, which lasted less than 30 minutes. The training sessions were kept short to keep the focus on how the device acutely altered their typical gait. The subjects began their training/acclimation session by walking overground and through handrails. Once the subject felt comfortable with the powered prosthesis, they began walking on the treadmill to allow more consecutive steps. Once the prosthesis was tuned for the individual and the subject could consistently

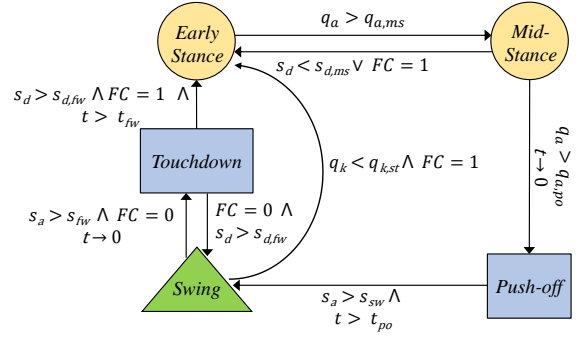


Fig. 2. Finite state machine representation of the proposed controller. The yellow circles correspond to impedance controlled states; the blue rectangles to time-based position controlled states; and the green triangle to the position control based on a holonomic phase variable.

walk without the use of handrails, the training session was concluded and recording trials began. During the treadmill walking trials, the subjects were encouraged to walk without the use of handrails, unless they felt unstable. There were a few trials when the subjects used the handrails during steady state walking, however we observed that they were mainly utilized for medial-lateral stabilization. Each subject walked on the treadmill for approximately 60 seconds with their day-to-day passive prosthesis and the powered prosthesis at their self-selected slow, normal, and fast walking speeds (Table II), resulting in a total of 6 walking trials. To determine the subject's self-selected normal speed, the treadmill speed was increased in increments of 0.1 m/s to the subjects satisfaction. The subject's fast and slow speeds were then set to 0.2 m/s above and below their normal speed.

While walking on the treadmill, the subjects wore a ceiling-mounted safety harness in case of trips or falls. Additionally, the subjects were given emergency stop buttons for both the treadmill and powered prosthesis, which they were instructed to press at any point if they felt the need to stop. Resting breaks were offered every 15 minutes, and were taken at any point the subject expressed fatigue. Lastly, the subjects were informed that they were allowed to opt-out of the experiment if at any point they felt uncomfortable.

### C. Control Method

The presented controller is based on a Finite State Machine (FSM), depicted in Fig. 2. The general structure of the FSM has been taken from [15], where a holonomic phase variable controller was designed to manage different rhythmic and non-rhythmic tasks. Although the presented controller is similar in structure, the control in each FSM state and the transition conditions between these states have changed.

Because mathematical singularities prevent a holonomic phase variable from performing optimally in the push-off and touchdown phases [15], these phases instead use time-based reference joint angle trajectories from normative able-bodied data [33], similar to [21]. While push-off, swing, and touchdown are all time-based in [21], our controller's swing period uses the holonomic phase variable method in [15]. This provides real-time synchronization to the user's walking speed

TABLE III

SPEED-INDEPENDENT CONTROL PARAMETERS. PARAMETERS  $K_p$  AND  $K_d$  ARE IN  $N \cdot m/rad$  AND  $N \cdot m \cdot s/rad$ , RESPECTIVELY.  $\theta_d$  IS IN  $rad$  AND IS NONCONSTANT WHEN NOTED AS TIME- OR PHASE-BASED, TB AND PB, RESPECTIVELY. PARAMETERS IN PARENTHESES ARE SPECIFIC TO TF3.

	Ankle			Knee		
	$K_p$	$K_d$	$\theta_d$	$K_p$	$K_d$	$\theta_d$
Early Stance	202 (246)	9 (11)	0	235 (286)	9 (11)	0.087
Midstance	812 (991)	9 (11)	0	235 (286)	9 (11)	0.087
push-off	563 (688)	14 (17)	TB	469 (573)	19 (23)	TB
Swing	563 (688)	14 (17)	PB	469 (573)	19 (23)	PB
Touchdown	202 (246)	9 (11)	TB	235 (286)	9 (11)	TB

TABLE IV  
SPEED-DEPENDENT CONTROL PARAMETERS

Subject	Speed	$q_h^{min}(rad)$	$q_{a,po}(rad)$	$t_{po}(s)$
TF1	Slow	-0.192	0.108	0.40
	Normal	-0.192	0.113	0.40
	Fast	-0.192	0.105	0.36
TF2	Slow	-0.192	0.108	0.40
	Normal	-0.192	0.106	0.40
	Fast	-0.192	0.105	0.36
TF3	Slow	-0.192	0.108	0.40
	Normal	-0.192	0.100	0.40
	Fast	-0.244	0.092	0.36

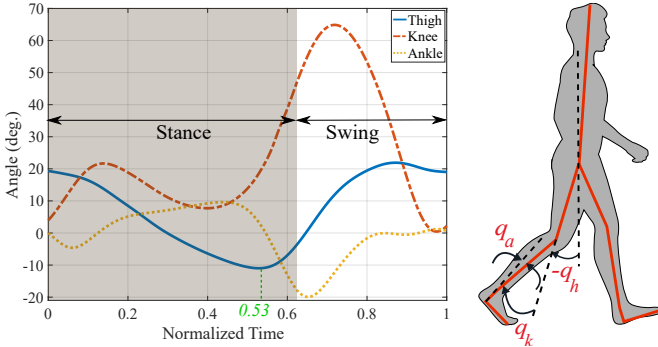


Fig. 3. Left: Human leg's joint angle trajectories during one stride of walking with normal speed and stride period  $T$  [33]. Right: Definition of the joint angles. Figure reproduced from [15].

and additional flexibility to perform non-rhythmic activities such as stepping over objects or kicking [15].

Another difference from the controller in [15] is the two states corresponding to the stance phase. We use an open-loop impedance controller for these states to take advantage of the low-impedance of the designed actuator. As we shown in [25], the designed actuator is capable of performing open-loop impedance control with small errors due to negligible unmodeled dynamics (e.g., friction and inertia). This means that biological quasi-stiffness values, reported in [34] and [35], can be applied without requiring torque feedback corrections. This can greatly shorten the parameter tuning sessions associated with open-loop impedance controllers, which tend to be very lengthy [36] since they must account for the actuator's unmodeled dynamics [25]. Note that these biological values were directly implemented for this experiment, and slightly reduced for the acclimation session. TF1 and TF2 kept the reduced values during the experimental trials, whereas TF3 preferred the original biological values (Table III).

Transitions in the FSM are based on foot contact ( $FC$ ) for stance states, time in time-based states, ankle angle for impedance-controlled states, and two phase variables for phase-controlled states. The phase variable  $s_d$  corresponding to touchdown and early stance, and the phase variable  $s_a$  corresponding to preswing and swing, are defined as in [15]:

$$s_d = \frac{q_h^0 - q_h}{q_h^0 - q_h^{min}} \cdot c, \quad s_a = 1 + \frac{1 - s_d}{q_h^0 - q_h^{min}} \cdot (q_h - q_h^0),$$

where  $q_h^0$  and  $q_h^{min}$  are constant values defined by touchdown thigh angle and the minimum of the reference thigh angle trajectory, respectively. These two parameters can be tuned to the individual's preference. The constant  $c$  is also tunable and is related to the ratio of the stance phase to the entire gait cycle. The default value of  $c$  is the normalized time at which  $q_h$  reaches its minimum, which is 0.53 in Fig. 3. The transitions are prescribed as follows:

1) *Transition between early and mid-stance*: When the ankle angle becomes greater than  $q_{a,ms}$ , the system will transition from early stance to mid-stance to accommodate more joint stiffness to prepare for push-off. Conversely, if the foot contact is lost or the thigh angle rises above  $s_d$ , the system goes back to early-stance, as the conditions for push-off preparation are not met.

2) *Transition from mid-stance to push-off*: When the ankle angle becomes greater than  $q_{a,po}$ , the transition to push-off occurs and time is set to zero. This is a one-way transition, i.e., the system cannot return to stance from the push-off state.

3) *Transition from push-off to swing*: As mentioned, push-off is a time-based state and as such, the instant of transition to swing is determined by the preset push-off duration ( $t_{po}$ ). To avoid premature transitions, the controller starts the swing phase only if, in addition to the duration condition, the thigh moves sufficiently forward and its angle reaches  $s_{sw}$ .

4) *Transition from swing to touchdown*: These transitions happen when the foot has not touched the ground yet, but a pre-specified forward (corresponding to  $s_{d,fw}$ ) thigh angle is reached. As mentioned, by transition to the touchdown state, the controller prepares the leg for a smooth touchdown.

5) *Transition from touchdown to (early) stance*: The touchdown state is time-based and thus the primary condition for this transition is the preset duration ( $t_{fw}$ ). The stance phase will start when the foot touches the ground ( $FC = 1$ ), however, only if the thigh angle has stayed above the previous limit (corresponding to  $s_{d,fw}$ ).

6) *Transition from touchdown to swing*: If the foot has not touched the ground and the absolute thigh angle becomes smaller than the values corresponding to  $s_{d,fw}$ , the FSM moves back to the swing phase. This will enable the user to perform volitional maneuvers while their leg is in the air, as we have previously shown in [15].

7) *Direct transition from swing to early stance*: This transition happens if the foot touches the ground during swing and the knee angle is smaller than some specified value.

Speed-independent control parameters that remained constant across subjects had the following values:  $q_h^0 = 0.367$  radians,  $q_{k,st} = 0.524$  radians,  $s_{fw} = 0.999$ ,  $s_{d,fw} = 0.1$ ,  $s_{d,ms} = 0.2$ ,  $s_{sw} = 0.65$ ,  $t_{fw} = 0.2$  seconds, and  $c = 0.53$ .

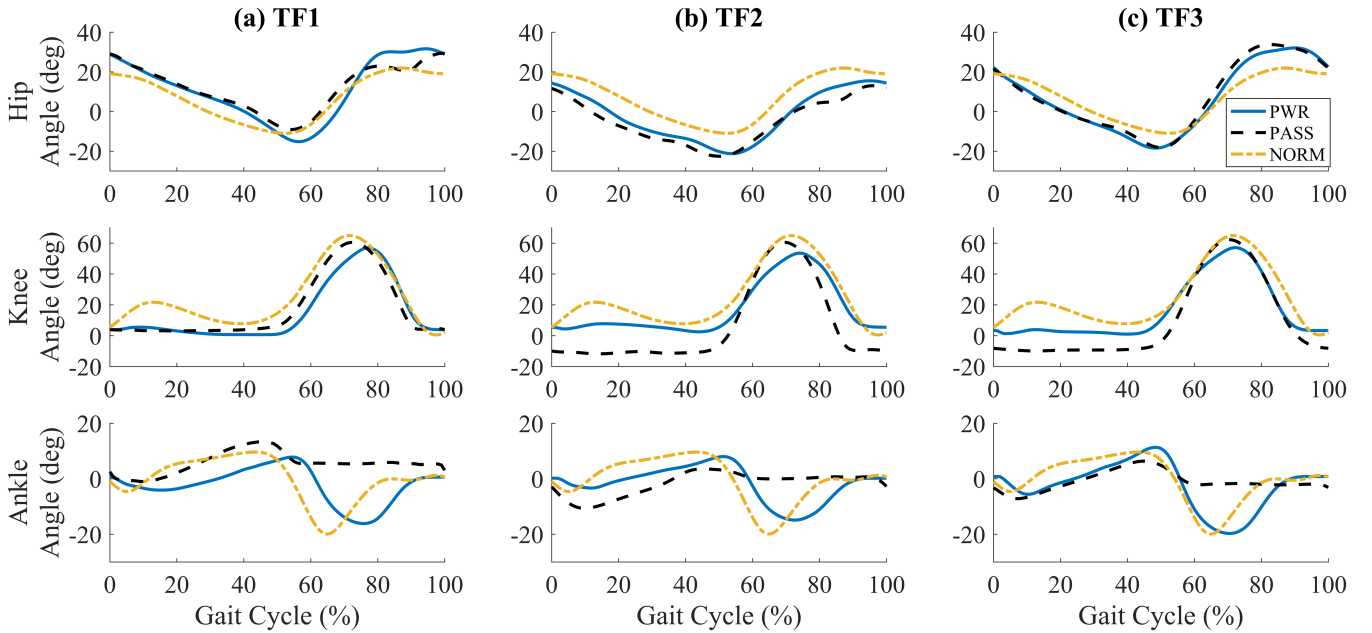


Fig. 4. Average prosthetic side joint kinematics at normal speeds throughout the gait cycle (normalized by time). Columns (a), (b), and (c) correspond to subjects TF1, TF2, and TF3, respectively. Top, middle, and bottom rows correspond to hip, knee, and ankle joint angles respectively. Solid blue lines indicate average angles for trials where the subject wore with the powered prosthesis (PWR), black dashed lines indicate trials where the subject wore their personal passive prosthesis (PASS), and dash-dotted yellow lines indicate healthy normative values (NORM) [33].

Other parameters that required slight tuning or vary with speed are shown in Tables III and IV, respectively.

#### D. Data Acquisition and Analysis

During walking trials, the subjects walked on an instrumented split-belt treadmill (Bertec, Columbus, OH, USA), which collected ground reaction forces at 1000 Hz. The subjects were outfitted with reflective markers (Fig. 1(b)) for lower body kinematics to be collected from our ten-camera motion capture system (Vicon, Oxford, UK) at 100 Hz. The conjunction of the instrumented treadmill and the motion capture system also allowed for lower-limb joint powers ( $W$ ) to be collected (100 Hz). Information relating to the powered prosthesis was saved on the myRIO at 500 Hz and used to determine the prosthetic joint power ( $W$ ). The collected dataset [37] and a supplemental multimedia file showing these experiments are available for download.

Positive, negative, and total joint work ( $J$ ) for the residual hip are calculated by taking the integral of positive values, negative values, and the absolute values of hip power (similar to [38], [39]), respectively. To measure circumduction, we begin by estimating each foot's center. This is done by averaging the location of all the markers on each foot. Circumduction is then defined by the lateral deviation of the foot center in mid-swing compared to stance, similar to [40]. Mid-swing is determined by the instant when the swing leg's foot center and crosses the stance leg's foot center during anterior-posterior motion. The lateral foot deviation is calculated for each step, then averaged for each subject, foot, and trial. Braking and propulsive impulses ( $N \cdot s/kg$ ) are found by integrating the positive and negative posterior-anterior ground reaction forces, respectively. An offset is subtracted from each trial's force data to compensate for drift caused by force measurement

integration errors over time. This offset is determined as the slope of the linear fit to the sum of the integrals of both leg's forces, which is then halved and subtracted from each leg's forces in the impulse calculation.

Throughout this paper, we use the symmetry index ( $SI$ ),

$$SI = \left| \frac{A - B}{\frac{1}{2}(A + B)} \right|, \quad (1)$$

to quantify symmetry between two quantities labeled  $A$  and  $B$  [15], [29], [41]. For example, when calculating the symmetry indices in Fig. 6 and Table V,  $A$  and  $B$  represent propulsive and braking impulses, respectively. Otherwise, in Tables VII and VIII,  $A$  and  $B$  represent values on the left and right legs, respectively. When  $SI = 0$ ,  $A$  and  $B$  are perfectly symmetric, whereas deviation from zero indicates increasing asymmetry.

### III. RESULTS

#### A. Transfemoral Amputee Subject 1

Maximum ankle plantarflexion returned to normative levels during powered trials, most notably at the push-off phase of gait ( $\sim 50\text{-}70\%$  GC), see Fig. 4(a). At slow speeds, ankle push-off power was higher with the powered prosthesis (Fig. 5(a)), but was similar in magnitude to the passive trials at normal and fast speeds. Although prosthetic ankle power did not increase for higher speeds when wearing the powered prosthesis, TF1 did exhibit increased prosthetic propulsive impulse across all speeds. This resulted in improved symmetry between braking and propulsive impulses for the powered prosthesis at all speeds, and for the intact side at the fast speed (Fig. 6(a)). Furthermore, the increase in prosthetic propulsive impulse resulted in improved symmetry between the prosthetic propulsive impulse and intact braking impulse, see Table V.

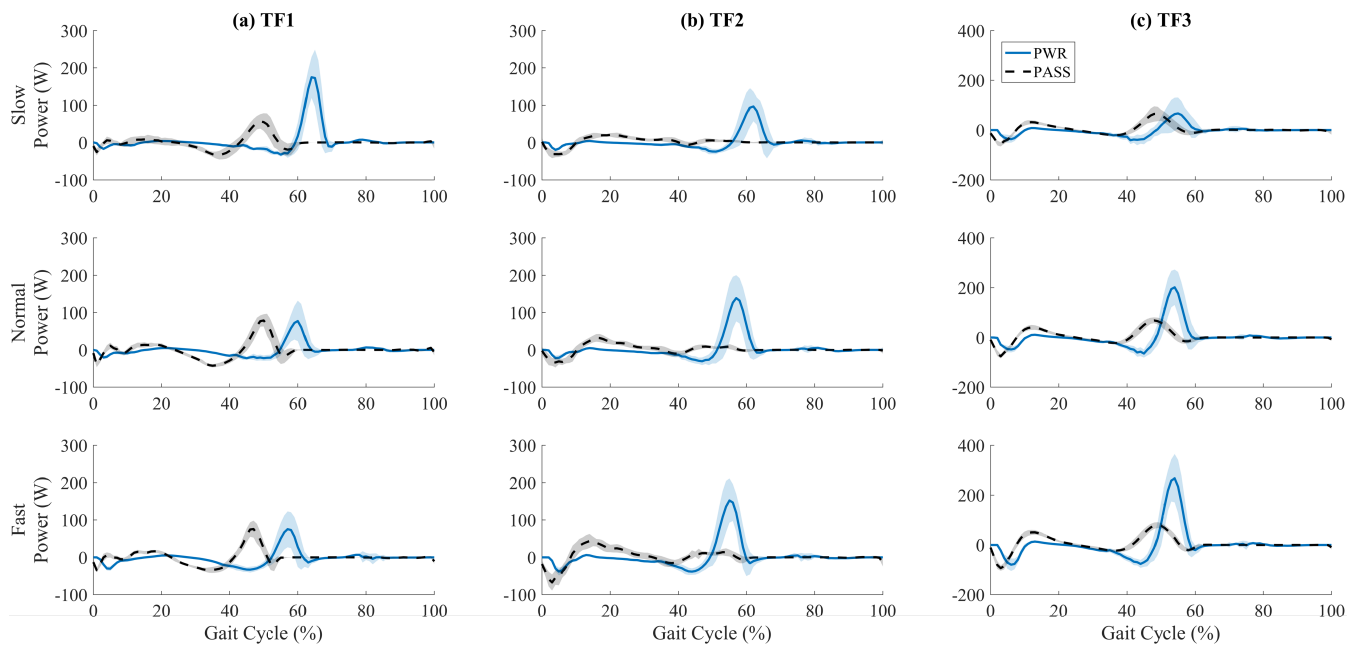


Fig. 5. Average prosthetic ankle power throughout the gait cycle (normalized by time). Columns (a), (b), and (c) correspond to subjects TF1, TF2, and TF3, respectively. Top, middle, and bottom rows correspond to slow, normal, and fast speeds, respectively. Solid blue lines indicate average power for trials where the subject wore with the powered prosthesis (PWR), and black dashed lines indicate trials where the subject wore their personal passive prosthesis (PASS). Shaded areas around the averages indicate  $\pm 1$  standard deviation.

TABLE V  
SYMMETRY INDEX BETWEEN PROSTHETIC PROPULSIVE IMPULSE AND INTACT BRAKING IMPULSE.

Subject	Speed	Powered	Passive
TF1	Slow	0.07	0.94
	Normal	0.23	0.68
	Fast	0.35	0.48
TF2	Slow	0.06	0.89
	Normal	0.11	1.20
	Fast	0.41	0.95
TF3	Slow	0.54	0.79
	Normal	0.43	0.81
	Fast	0.40	0.72

TABLE VI  
AVERAGE POSITIVE (+), NEGATIVE (-), AND TOTAL HIP MECHANICAL WORK PER STRIDE IN JOULES FOR THE RESIDUAL LIMB.

Subject	Speed	Powered			Passive		
		(+)	(-)	Total	(+)	(-)	Total
TF1	Slow	10.5	14.6	25.0	10.5	25.8	36.3
	Normal	13.6	23.1	36.8	12.2	33.7	45.9
	Fast	10.8	21.2	32.0	9.9	28.2	38.1
TF2	Slow	8.7	10.3	19.0	10.8	13.7	24.5
	Normal	10.4	14.2	24.6	14.0	16.1	30.2
	Fast	13.6	22.7	36.4	15.9	22.0	37.9
TF3	Slow	29.6	65.0	94.6	29.5	66.3	95.8
	Normal	29.1	70.0	99.0	31.8	78.5	110.4
	Fast	34.1	74.0	108.1	34.8	81.8	116.6

Beginning at early stance ( $\sim 0$ -10% GC) of the passive trials, TF1 exhibited a large spike in positive residual hip power, see Fig. 7(a). This behavior was mitigated when walking with the powered prosthesis. Furthermore, a large reduction in residual hip negative power is evident at late stance ( $\sim 45$ % GC) for all speeds of the powered trials. Across speeds, the residual hip had more concentric pull-off power with the powered prosthesis, as seen in Fig. 7(a) at  $\sim 65$ -70% GC. This increase was less noticeable at slow speeds, which had more prosthetic ankle push-off power. During passive trials, TF1 displayed a

TABLE VII  
AVERAGE STEP LENGTH IN  $mm$ , AND SYMMETRY INDEX (SI) COMPARING THE LEFT AND RIGHT FOOT DURING POWERED AND PASSIVE TRIALS.

Subject	Speed	Powered			Passive		
		Left	Right	SI	Left	Right	SI
TF1	Slow	824	744	0.10	531	582	0.09
	Normal	843	798	0.06	672	721	0.07
	Fast	777	839	0.08	756	784	0.04
TF2	Slow	672	667	0.01	600	656	0.09
	Normal	694	715	0.03	636	702	0.10
	Fast	716	756	0.06	675	749	0.10
TF3	Slow	652	707	0.08	608	669	0.10
	Normal	696	745	0.07	683	748	0.09
	Fast	747	800	0.07	718	791	0.10

TABLE VIII  
HIP CIRCUMDUCTION DEFINED BY AVERAGE LATERAL FOOT DEVIATION IN  $mm$ . SYMMETRY INDEX (SI) COMPARING THE LEFT AND RIGHT FOOT DURING POWERED AND PASSIVE TRIALS.

Subject	Speed	Powered			Passive		
		Left	Right	SI	Left	Right	SI
TF1	Slow	54	15	1.12	68	28	0.84
	Normal	74	8	1.58	87	15	1.43
	Fast	80	3	1.86	85	13	1.48
TF2	Slow	43	13	1.09	-4	-2	0.56
	Normal	52	-4	2.36	13	3	1.24
	Fast	50	-9	2.89	-6	-5	0.22
TF3	Slow	-9	19	5.78	-20	17	18.91
	Normal	-6	22	3.54	-36	19	6.15
	Fast	8	25	1.00	-37	21	7.61

large magnitude oscillation between positive and negative hip power at the end of prosthetic swing ( $\sim 90$ % GC), resulting in rapid hip flexion/extension (see Fig. 4(a)). These oscillations in hip flexion/extension and power were not seen in powered trials. Note that although oscillations in hip flexion/extension were mitigated in powered trials, peak flexion during this stage of gait is larger than passive trials and normative values. Lastly, TF1 experienced a slight increase in positive residual hip work,

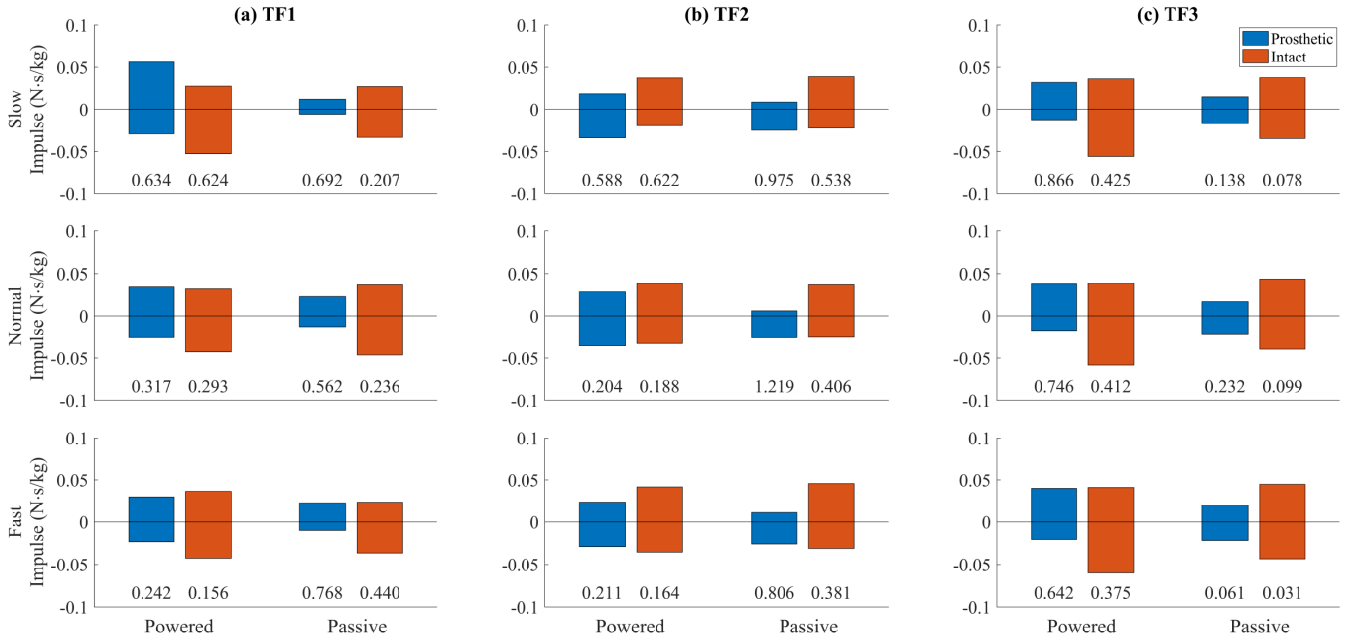


Fig. 6. Average propulsive (positive) and braking (negative) impulses when walking with the powered and passive prostheses. Columns (a), (b), and (c) correspond to subjects TF1, TF2, and TF3, respectively. Top, middle, and bottom rows correspond to slow, normal, and fast speeds, respectively. Within each sub-figure, the bars are paired depending on the prosthesis worn. Corresponding symmetry indices between average propulsive and braking impulses for each individual side are shown below each set of bars.

and a decrease in negative residual hip work, when wearing the powered prosthesis. This led to a 22% average decrease in total residual hip work with the powered prosthesis (Table VI).

Aside from gait kinetics, we also examined how the powered prosthesis affects other compensatory behaviors related to step length and hip circumduction. When wearing the powered prosthesis, TF1 displayed an increased step length on both the prosthetic and intact side at all speeds (Table VII). Furthermore, symmetry between the left and right step length was improved for normal speeds. Although symmetry decreased for slow and fast speeds, the difference in  $SI$  was very small ( $\sim 0.01$  and  $0.04$ , respectively). TF1 also exhibited reduced hip circumduction at all speeds (Table VIII), though the  $SI$  between the left and right sides increased.

### B. Transfemoral Amputee Subject 2

During the passive trials, TF2 displayed very little prosthetic ankle push-off power and plantarflexion. The powered prosthesis drastically increased ankle push-off power and plantarflexion across all speeds in Fig. 5(b) and Fig. 4(b). TF2's gait also had larger prosthetic propulsive impulse across all speeds during powered trials, see Fig. 6(b). This resulted in improved symmetry between braking and propulsive impulses for both the prosthetic and intact sides, except for the intact leg at slow speeds. Furthermore, the increase in prosthetic propulsive impulse resulted in improved symmetry between the prosthetic propulsive impulse and the intact braking impulse.

Across all speeds, TF2 had reduced peak-to-peak residual hip power when wearing the powered prosthesis (Fig. 7(b)). TF2 exhibited a decrease in peak negative prosthetic-side hip power during powered trials at  $\sim 30$ -50% GC. Concentric pull-off power, occurring  $\sim 50$ -65% GC, was also reduced in

powered trials. Similar to TF1, TF2 displayed oscillation between positive and negative hip power at the end of prosthetic swing ( $\sim 90\%$  GC) during passive trials, resulting in rapid hip flexion/extension (see Fig 4(b)). This behavior was mitigated with the powered prosthesis. Otherwise, hip kinematics are fairly similar to passive trials, though both cases are shifted  $\sim 5$ -10° lower than normative hip kinematics. Lastly, TF2 experienced reduced positive residual hip work at all speeds with the powered prosthesis. Negative hip work was also decreased during slow and normal trials, and slightly increased during fast walking. The combination of positive and negative hip work resulted in a 15% average reduction of total residual hip work when wearing the powered prosthesis (Table VI).

In all speeds of the powered trials, TF2 displayed increased step length on both sides (Table VII). Furthermore, the symmetry between left and right step lengths were increased for all speeds. During passive trials, TF2 displayed little hip circumduction for both the prosthetic and intact side, see Table VIII. They did, however, present abnormal behavior during slow and fast trials, where the foot measured a negative circumduction during the swing phase. This may be caused by excessive lateral sway of the trunk or abnormal swing leg kinematics. The powered prosthesis mitigated these trends for the prosthetic side but resulted in an increased circumduction that was larger than healthy averages [40]. Furthermore, this increased circumduction resulted in increased  $SI$ .

### C. Transfemoral Amputee Subject 3

Similar to the other subjects, TF3's prosthetic ankle plantarflexion returned to normative levels when wearing the powered prosthesis (Fig. 4(c)). Prosthetic push-off power was also drastically increased for normal and fast speeds when wearing the powered prosthesis, see Fig. 5(c). At slow speeds,

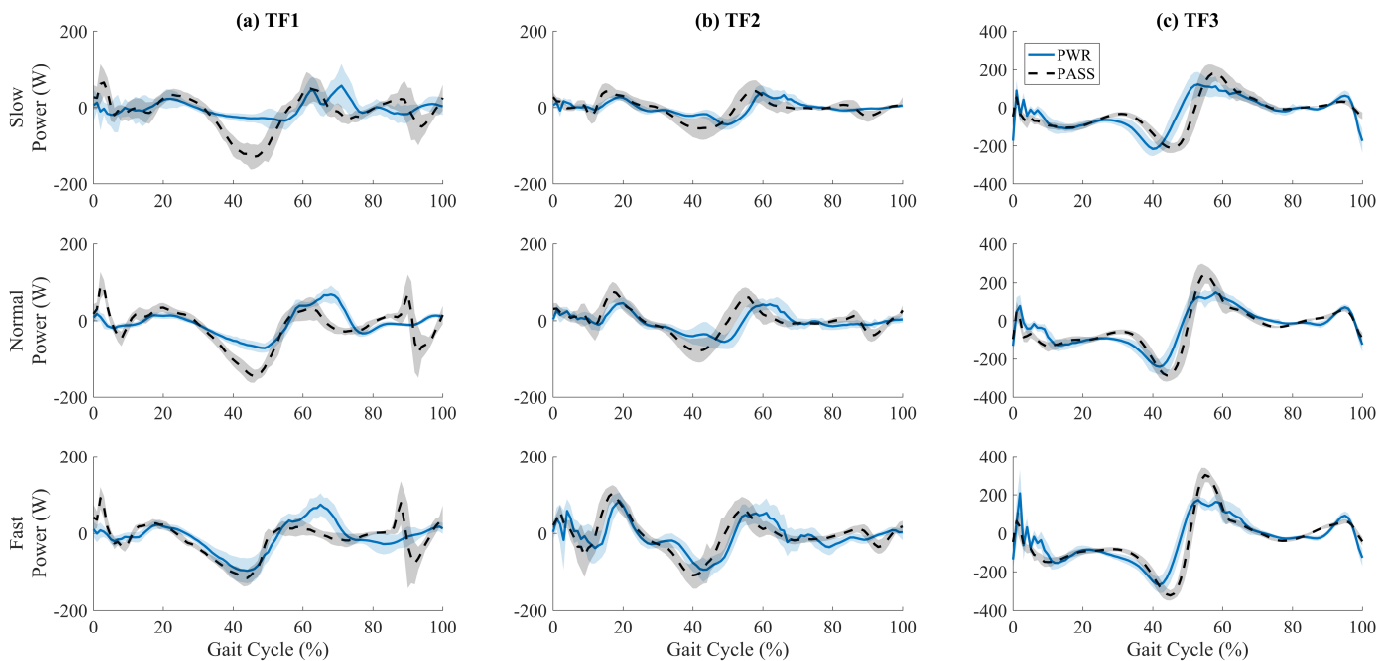


Fig. 7. Average prosthetic side hip power throughout the gait cycle (normalized by time). Columns (a), (b), and (c) correspond to subjects TF1, TF2, and TF3, respectively. Top, middle, and bottom rows correspond to slow, normal, and fast speeds, respectively. Solid blue lines indicate average power for trials where the subject wore with the powered prosthesis (PWR), and black dashed lines indicate trials where the subject wore their personal passive prosthesis (PASS). Shaded areas around the averages indicate  $\pm 1$  standard deviation.

peak push-off power was similar to that of the passive device. TF3 displayed an increase in prosthetic propulsive impulse when wearing the powered prosthesis (Fig. 6(c)). Wearing the powered prosthesis resulted an increased symmetry index between propulsive and braking impulses of the prosthetic and intact leg. Although TF3 exhibited an increased braking impulse on their intact leg, the increased prosthetic leg propulsive impulse led to improved symmetry between the two, compared to the passive trials (Table V).

Similar to TF2, TF3 had reduced peak-to-peak residual hip power during powered trials (Fig. 7(c)). Negative peaks at  $\sim 45\%$  GC were reduced at normal and fast speeds. Positive concentric pull-off powers at  $\sim 50\text{-}60\%$  GC were drastically reduced during powered trials. Although positive hip work was slightly increased for slow walking with the powered prosthesis (by 0.1 J), it decreased by larger amounts in normal and fast trials (Table VI). Furthermore, negative hip work was reduced for all speeds. These reductions led to a 6% average decrease in total residual hip work. This seemed to have little effect on hip kinematics, and a notable deviation from normative hip kinematics, namely flexion prior to ground impact, was observed with both prostheses. This deviation was slightly reduced during powered trials.

During powered trials, TF3 displayed an increased step length for both the prosthetic and intact side, for all speeds (Table VII). The only exception is at normal speed, where the intact leg had a decreased step length. However this decrease was on average only 4mm, which is negligible. Nevertheless, the step length's *SI* was decreased for all speeds, indicating improved symmetry. During passive trials, TF3 displayed a similar abnormality to TF2, which resulted in a negative circumduction for the prosthetic leg (Table VIII). Although this was not completely mitigated when walking on the powered

prosthesis, it was greatly reduced, and even averaged positive and normative values at their fast speed [40]. The intact leg's circumduction increased, but only slightly, which resulted in improved symmetry across all speeds.

#### IV. DISCUSSION

Knee and ankle kinematics had more normative characteristics for the powered leg than the passive leg [33]. Similar to other powered prostheses, the prosthetic ankle was able to achieve much more plantarflexion compared to the passive ankles. The powered prosthetic knee maintained normative levels of flexion during swing, and reduced the stance knee hyperextension (TF2 and TF3) that commonly occurs in amputee gait to ensure knee stability. The powered knee angles varied during stance instead of being locked during most of this period. We suspect that more extensive tuning and training could allow knee flexion to resemble normative values even more closely than presented here. Hip range-of-motion was similar between passive and powered trials for each subject. However, deviations from normative trends were evident in TF1 and TF2 passive trials, namely in the rapid flexion and extension of the residual hip during late swing. This motion was coupled with rapid oscillation between positive and negative hip power, which was most likely caused by the lack of knee control during swing. This compensation was greatly mitigated with the powered leg, implying greater control of the knee during swing. TF3 exhibited deviations from normative hip kinematics with both the powered and passive prostheses, which was only slightly reduced during powered trials. Otherwise, hip kinematics were not greatly altered between powered and passive trials.

Stride length is typically reduced in transfemoral amputee gait [42] as a method of compensation for less precise leg

function [29]. However, passive and powered prostheses that can release/inject energy during push-off have shown to reduce this compensation [43]. Our results follow this trend: the step length of the prosthetic and intact leg were increased for almost every powered trial, averaging an increase of  $\sim 60$  mm for the prosthetic and intact leg. In many cases, step length returned to normative levels ( $\sim 740$ - $820$ mm) [40], improving symmetry between the prosthetic and intact side. Stance time symmetry and swing time symmetry between the right and left legs improved for TF1 and TF2, but worsened for TF3. Temporal variables could potentially be improved by further tuning the timing parameters of the controller.

Across all speeds and subjects, propulsive impulses were increased when walking with the powered prosthesis. This can be attributed to active injection of power and increased step length. An increased step length allows greater posterior travel of the prosthetic foot during the stance phase, which results in larger push-off power to contribute to forward propulsion. In addition to increased propulsive impulses with the powered prosthesis, all subjects displayed improved symmetry between the propulsive impulse of the prosthesis and the braking impulse of the intact leg. This is particularly important because asymmetry between these two impulses often force the hip to implement costly strategies [30], i.e., increased concentric hip work to compensate for missing ankle push-off work [23]. However, this hip compensation is insufficient to fully replace the missing ankle push-off work [7]. Therefore, we suggest that the increased impulse produced by our powered prosthesis can contribute to reduced residual hip power.

We also saw how the utilization of the prosthesis can vary between subjects when looking at the prosthetic push-off power. TF1 typically preferred shorter steps, which led to premature removal of the prosthetic foot from the ground when entering the swing phase. This resulted in similar push-off power between the powered leg and their passive leg. Consequently, this subject's residual hip exhibited higher concentric pull-off power ( $\sim 70\%$  GC) to lift the heavier prosthesis into swing. On the other hand, TF2 and TF3 exploited the capabilities of the powered prosthesis to greatly increase their prosthetic ankle push-off. Reductions in concentric hip pull-off power are evident for these subjects, reducing positive residual hip work in all but one trial. This observation suggests that concentric hip pull-off power is directly related to the lack of prosthetic ankle push-off power in amputee gait [23], [44]. Therefore, compensatory power production at the residual hip can potentially be reduced by powered prostheses that can produce large ankle push-off power followed by fast ankle/knee flexion.

Circumduction is another compensation commonly seen in amputee gait to provide toe-clearance for the prosthetic foot. Circumduction can be caused by the lack of dorsiflexion in passive prosthetic ankles and swing control in passive knees. Powered prostheses can help reduce this compensation by actively controlling the joint angles. However, powered prostheses with high-impedance actuators have difficulty transitioning between large plantarflexion push-off power at the ankle and high-speed flexion at the ankle and knee to provide sufficient toe-clearance [15]. We hypothesized that the increased position

and force bandwidth that is inherent to this style of actuation [25]–[27] would reduce this compensation. Circumduction was reduced for both the prosthetic and intact limbs during the powered trials of TF1. Although circumduction was only reduced on the prosthetic side for TF3, symmetry was substantially improved between the prosthetic and intact limb. On the other hand, TF2 did not exhibit much circumduction from the beginning, and prosthetic circumduction increased when wearing the powered prosthesis. Hence, the potential benefits with respect to circumduction appear to depend on the subject.

Although this study did not focus on intact limb compensations, it should be noted that one subject (TF1) exhibited ankle vaulting when walking with both prostheses. Preliminary analysis suggests that this compensation became slightly worse with the powered prosthesis, although vaulting was not necessary to facilitate toe clearance. An additional investigation would be necessary to determine whether this was a reaction to walking with an unfamiliar device. The study participants only had a brief acclimation period (about 30 minutes) with the powered prosthesis before data collection. It is possible that more extensive training is needed to mitigate many amputee compensations, which have been learned over a long period of time using their conventional prosthesis.

## V. CONCLUSION

The increased power and bandwidth available in the low-impedance powered prosthesis have the potential to reduce amputee compensations at the residual hip compared to use of conventional passive prostheses. This case series demonstrates that the amount of push-off power a subject receives depends on how they walk on the prosthesis. When correctly utilized, the powered prosthesis drastically increased the ankle push-off power, resulting in reduced residual hip pull-off power. Increased push-off power, coupled with an increase in step length, resulted in an increased propulsive impulse on the prosthetic side for all subjects. All subjects displayed improved symmetry between the prosthetic propulsive impulse and the intact braking impulse, which has been linked to compensatory work at the residual hip. The combination of the reduced compensations at the hip resulted in a  $\sim 13\%$  average reduction in total residual hip work per stride. Although metabolic energy expenditure was not collected, the decreased work at the residual hip suggests the same task can be performed at a reduced cost [31], which could allow for extended periods of daily ambulation and lead to improved quality of life. Furthermore, although this study does not include analysis with other powered prostheses, the powered prosthesis used in this study is described in great detail and compared against several other powered prostheses in [25].

The powered prosthesis also reduced hip circumduction in subjects who exhibited large circumduction with their passive prosthesis, whereas circumduction increased for the subject who did not exhibit this compensation from the start. Therefore, potential benefits with respect to circumduction may depend on the subject. Additional investigations are needed to determine whether hip circumduction can be more consistently reduced with this prosthesis when given additional training.

## ACKNOWLEDGMENT

The authors thank Kyle Embry, Lizbeth Zamora, Edgar Bolivar and Mark Yeatman for their experimental assistance.

## REFERENCES

- [1] D. A. Winter and S. E. Sienko, "Biomechanics of below-knee amputee gait," *Journal of biomechanics*, vol. 21, no. 5, pp. 361–367, 1988.
- [2] K. R. Kaufman, S. Frittoli, and C. A. Frigo, "Gait asymmetry of transfemoral amputees using mechanical and microprocessor-controlled prosthetic knees," *Clinical Biomech.*, vol. 27, no. 5, pp. 460–465, 2012.
- [3] D. Berry, "Microprocessor prosthetic knees," *Phys. Med. Rehabil. Clin.*, vol. 17, no. 1, pp. 91–113, 2006.
- [4] C. L. Lewis and D. P. Ferris, "Walking with increased ankle pushoff decreases hip muscle moments," *Journal of biomechanics*, vol. 41, no. 10, pp. 2082–2089, 2008.
- [5] H. M. Herr and A. M. Grabowski, "Bionic ankle-foot prosthesis normalizes walking gait for persons with leg amputation," *Proc. of the Royal Society B: Biol. Sciences*, vol. 279, no. 1728, pp. 457–464, 2011.
- [6] R. Gailey, K. Allen, J. Castles, J. Kucharik, and M. Roeder, "Review of secondary physical conditions associated with lower-limb amputation and long-term prosthesis use," *J. Rehabil. Res. Dev.*, vol. 45, no. 1, 2008.
- [7] A. K. Silverman, N. P. Fey, A. Portillo, J. G. Walden, G. Bosker, and R. R. Neptune, "Compensatory mechanisms in below-knee amputee gait in response to increasing steady-state walking speeds," *Gait & posture*, vol. 28, no. 4, pp. 602–609, 2008.
- [8] D. G. Smith, J. W. Michael, and J. H. Bowker, Eds., *Atlas of Amputations and Limb Deficiencies: Surgical, Prosthetic, and Rehabil. Principles*. Rosemont, IL: American Academy of Orthopaedic Surgeons, 2004.
- [9] D. E. Hurwitz, D. R. Sumner, and J. A. Block, "Bone density, dynamic joint loading and joint degeneration," *Cells Tissues Organs*, vol. 169, no. 3, pp. 201–209, 2001.
- [10] D. Norvell, J. Czerniecki, G. Reiber, C. Maynard, J. Pecoraro, and N. Weiss, "The prevalence of knee pain and symptomatic knee osteoarthritis among veteran traumatic amputees and nonamputees," *Arch. Phys. Med. Rehabil.*, vol. 86, no. 3, pp. 487–493, 2005.
- [11] J. Kulkarni, W. Gaine, J. Buckley, J. Rankine, and J. Adams, "Chronic low back pain in traumatic lower limb amputees," *Clinical rehabilitation*, vol. 19, no. 1, pp. 81–86, 2005.
- [12] D. S. Pieringer, M. Grimmer, M. F. Russold, and R. Riener, "Review of the actuators of active knee prostheses and their target design outputs for activities of daily living," in *IEEE Int. Conf. Rehabil. Robot.*, 2017, pp. 1246–1253.
- [13] M. A. Price, P. Beckerle, and F. C. Sup IV, "Design optimization in lower limb prostheses: A review," *IEEE Trans. Neural Sys. Rehab. Eng.*, 2019.
- [14] B. Laschowski, J. McPhee, and J. Andrysek, "Lower-limb prostheses and exoskeletons with energy regeneration: Mechatronic design and optimization review," *J. Mechanisms and Robotics*, vol. 11, no. 4, 2019.
- [15] S. Rezazadeh, D. Quintero, N. Divekar, E. Reznick, L. Gray, and R. D. Gregg, "A phase variable approach for improved rhythmic and non-rhythmic control of a powered knee-ankle prosthesis," *IEEE Access*, vol. 7, pp. 109 840–109 855, 2019.
- [16] D. Quintero, E. Reznick, D. J. Lambert, S. Rezazadeh, L. Gray, and R. D. Gregg, "Intuitive clinician control interface for a powered knee-ankle prosthesis: A case study," *IEEE J. Trans. Eng. in Health and Medicine*, vol. 6, pp. 1–9, 2018.
- [17] D. C. Morgenroth, A. D. Segal, K. E. Zelik, J. M. Czerniecki, G. K. Klute, P. G. Adamczyk, M. S. Orendurff, M. E. Hahn, S. H. Collins, and A. D. Kuo, "The effect of prosthetic foot push-off on mechanical loading associated with knee osteoarthritis in lower extremity amputees," *Gait & posture*, vol. 34, no. 4, pp. 502–507, 2011.
- [18] C. Jayaraman *et al.*, "Impact of powered knee-ankle prosthesis on low back muscle mechanics in transfemoral amputees: A case series," *Frontiers in neuroscience*, vol. 12, p. 134, 2018.
- [19] D. Quintero, D. J. Villarreal, D. J. Lambert, S. Kapp, and R. D. Gregg, "Continuous-phase control of a powered knee-ankle prosthesis: Amputee experiments across speeds and inclines," *IEEE Transactions on Robotics*, vol. 34, no. 3, pp. 686–701, 2018.
- [20] T. Lenzi, M. Cempini, L. Hargrove, and T. Kuiken, "Design, development, and validation of a lightweight non-backdrivable robotic ankle prosthesis," *IEEE/ASME Transactions on Mechatronics*, 2019.
- [21] B. E. Lawson, J. Mitchell, D. Truex, A. Shultz, E. Ledoux, and M. Goldfarb, "A robotic leg prosthesis: Design, control, and implementation," *IEEE Robotics & Automation Magazine*, vol. 21, no. 4, pp. 70–81, 2014.
- [22] M. Tran, L. Gabert, M. Cempini, and T. Lenzi, "A lightweight, efficient fully-powered knee prosthesis with actively variable transmission," *IEEE Robotics and Automation Letters*, 2019.
- [23] R. E. Seroussi, A. Gitter, J. M. Czerniecki, and K. Weaver, "Mechanical work adaptations of above-knee amputee ambulation," *Arch. of Physical Medicine and Rehabil.*, vol. 77, no. 11, pp. 1209–1214, 1996.
- [24] T. Elery, S. Rezazadeh, C. Nesler, J. Doan, H. Zhu, and R. D. Gregg, "Design and benchtop validation of a powered knee-ankle prosthesis with high-torque, low-impedance actuators," in *IEEE Int. Conf. Robot. Automat.*, 2018.
- [25] T. Elery, S. Rezazadeh, C. Nesler, and R. D. Gregg, "Design and validation of a powered knee-ankle prosthesis with high-torque, low-impedance actuators," *IEEE Trans. Robotics*, 2020.
- [26] S. Seok, A. Wang, M. Y. M. Chuah, D. J. Hyun, J. Lee, D. M. Otten, J. H. Lang, and S. Kim, "Design principles for energy-efficient legged locomotion and implementation on the mit cheetah robot," *IEEE/ASME Transactions on Mechatronics*, vol. 20, no. 3, pp. 1117–1129, 2015.
- [27] H. Zhu, C. Nesler, N. Divekar, M. T. Ahmad, and R. D. Gregg, "Design and validation of a partial-assist knee orthosis with compact, backdrivable actuation," in *IEEE Int. Conf. Rehabil. Robot.*, 2019.
- [28] R. J. Zmitrowicz, R. R. Neptune, J. G. Walden, W. E. Rogers, and G. W. Bosker, "The effect of foot and ankle prosthetic components on braking and propulsive impulses during transtibial amputee gait," *Arch. of Physical Medicine and Rehabil.*, vol. 87, no. 10, pp. 1334–1339, 2006.
- [29] M. Schaarschmidt, S. W. Lipfert, C. Meier-Gratz, H.-C. Scholle, and A. Seyfarth, "Functional gait asymmetry of unilateral transfemoral amputees," *Human movement science*, vol. 31, no. 4, pp. 907–917, 2012.
- [30] H. Houdijk, E. Pollmann, M. Groenewold, H. Wiggerts, and W. Polomski, "The energy cost for the step-to-step transition in amputee walking," *Gait & posture*, vol. 30, no. 1, pp. 35–40, 2009.
- [31] K. Sasaki, R. R. Neptune, and S. A. Kautz, "The relationships between muscle, external, internal and joint mechanical work during normal walking," *J. Exp. Biol.*, vol. 212, no. 5, pp. 738–744, 2009.
- [32] R. G. Burdett, G. S. Skrinar, and S. R. Simon, "Comparison of mechanical work and metabolic energy consumption during normal gait," *Journal of orthopaedic research*, vol. 1, no. 1, pp. 63–72, 1983.
- [33] D. A. Winter, *Biomechanics and Motor Control of Human Movement*, 2nd ed. New York, NY: Wiley, 2009.
- [34] K. Shamaei, G. S. Sawicki, and A. M. Dollar, "Estimation of quasi-stiffness of the human knee in the stance phase of walking," *PloS one*, vol. 8, no. 3, p. e59993, 2013.
- [35] —, "Estimation of quasi-stiffness and propulsive work of the human ankle in the stance phase of walking," *PloS one*, vol. 8, no. 3, p. e59935, 2013.
- [36] A. M. Simon, K. A. Ingraham, N. P. Fey, S. B. Finucane, R. D. Lipschutz, A. J. Young, and L. J. Hargrove, "Configuring a powered knee and ankle prosthesis for transfemoral amputees within five specific ambulation modes," *PLOS ONE*, vol. 9, no. 6, pp. 1–10, 06 2014.
- [37] T. Elery, S. Rezazadeh, E. Reznick, L. Gray, and R. Gregg, "Effects of a powered knee-ankle prosthesis on amputee hip compensations: A case series," *IEEE DataPort*, 2020. [Online]. Available: <http://dx.doi.org/10.21227/sngq-4x29>.
- [38] I. Chen, K. Kuo, and T. Andriacchi, "The influence of walking speed on mechanical joint power during gait," *Gait & Posture*, vol. 6, no. 3, pp. 171–176, 1997.
- [39] L. F. Teixeira-Salmela, S. Nadeau, M.-H. Milot, D. Gravel, and L. F. Requião, "Effects of cadence on energy generation and absorption at lower extremity joints during gait," *Clin. Biomech.*, vol. 23, no. 6, pp. 769–778, 2008.
- [40] K. A. Shorter, A. Wu, and A. D. Kuo, "The high cost of swing leg circumduction during human walking," *Gait & posture*, vol. 54, pp. 265–270, 2017.
- [41] K. K. Patterson, W. H. Gage, D. Brooks, S. E. Black, and W. E. McIlroy, "Evaluation of gait symmetry after stroke: a comparison of current methods and recommendations for standardization," *Gait & posture*, vol. 31, no. 2, pp. 241–246, 2010.
- [42] R. Waters, J. Perry, D. Antonelli, and H. Hislop, "Energy cost of walking of amputees: the influence of level of amputation," *J. Bone Joint Surg. Am.*, vol. 58, no. 1, pp. 42–46, 1976.
- [43] B. E. Lawson, B. Ruhe, A. Shultz, and M. Goldfarb, "A powered prosthetic intervention for bilateral transfemoral amputees," *IEEE Transactions on Biomedical Engineering*, vol. 62, no. 4, pp. 1042–1050, 2014.
- [44] S. W. Lipfert, M. Gunther, D. Renjewski, and A. Seyfarth, "Impulsive ankle push-off powers leg swing in human walking," *Journal of experimental biology*, vol. 217, no. 8, pp. 1218–1228, 2014.